

Evaluation of Surface Preparation Technology for Steel Components with Fluoropolymer-Based Coatings in Terms of Anti-Adhesive and Mechanical Properties

Izabela Miturska-Barańska^{1*}, Elżbieta Doluk¹

¹ Lublin University of Technology, Faculty of Mechanical Engineering, Nadbystrzycka 36, 20-618 Lublin, Poland

* Corresponding author's e-mail: i.miturska@pollub.pl

ABSTRACT

The subject of the research presented in this paper was the evaluation of the technology of surface preparation of steel samples in terms of anti-adhesion and mechanical properties through the use of PFA coatings. Such coatings are used in many industries, e.g. in the manufacture and operation of metal moulds used, for example, in the production of resinous components. The specimens used in the study, which represented the surface of the moulds, were made from DC01 sheet. Six variants of release coating technology were used, differing in the number of technological operations and parameters. In the final stage, appropriate test methods were used to assess the energy properties of the coatings produced, the mechanical properties in terms of deformation of the supporting structure and the mechanical properties in terms of the effects on the coating itself. The scope of the research made it possible to determine the main properties that the manufactured coatings have in terms of their future practical applications. The results obtained for the surface free energy determined from the measurement of the surface wetting angle, the mechanical properties obtained from the three-point bending test and the evaluation of the surface quality of the coatings subjected to compressive and tensile deformations in the bending test, as well as the functional properties of the coatings in terms of their durability and adhesion determined in scratch tests, showed that the best characteristics were obtained for variant 6. This variant consisted of sequentially, after the initial stage, applying a primer layer and drying it for 15 minutes at 250 °C, applying a PFA layer to the component at 150 °C and then drying it for 15 minutes at 200 °C and curing it for 20 minutes at 380 °C. An additional layer of PFA was then applied and dried for 15 minutes at 200 °C and cured for 20 minutes at 340 °C. In addition, a long annealing for 3 hours at 340 °C was applied in a given variant.

Keywords: anti-adhesive properties, PFA coating, surface free energy, three-point bending, scratch tests.

INTRODUCTION

The production of barrier coatings that modify the characteristics of the surface layer is an issue that is still being addressed and developed by the scientific community [1–3]. In addition, it has a wide range of practical applications in all industries, including aerospace, automotive, electrical and energy, as well as in the food, medical, chemical and wider manufacturing industries [4–10]. Barrier coatings can be made from a variety of materials, depending on their purpose and the specific function they are intended to perform. Examples of barrier coating materials are:

metals, polymers, ceramics, block copolymers, nanomaterials or resins [11–13]. Polymeric coatings in particular deserve recognition because they are considered versatile and can be individually adapted to meet the requirements placed on them. According to coating manufacturers and many authors, polymeric coatings can be applied to various substrates, i.e. stainless steel, low-alloy steel, aluminium alloys, brass, glass, ceramics and some types of rubber and plastics [5, 6, 14–17].

Polymer coatings, are also known as anti-adhesive, release or demoulding coatings. Despite the well-known chemical composition of polymer coatings, there are still some challenges in

this aspect. According to Paz-Gómez et al. [1] it is important to investigate aspects such as the durability of coatings and optimal deformation. As outlined in their publication by Schellenberger et al. [18] anti-adhesive coatings allow easy removal of liquids from their surface and can be described as superhydrophobic when its wetting angle is greater than 150° . According to Liu, Fürstner and co-authors [19, 20] low-adhesion surfaces also exhibit various properties, such as self-cleaning.

The production of anti-adhesive coatings is the process of manufacturing special coatings using a number of different polymeric materials. The materials most commonly used in the production of release coatings and also of greatest importance are:

- PTFE coatings (polytetrafluoroethylene) have excellent non-stick properties, a high working temperature of up to 260°C , an extremely low coefficient of friction and good abrasion resistance [21–23].
- PFA coatings (perfluoroalkoxy polymer) are characterised by very good non-stick properties, a high operating temperature of up to 260°C , high coating thicknesses of up to $300\ \mu\text{m}$ and excellent chemical resistance [24, 25].
- FEP coatings (tetrafluoroethylene/fluoropropylene copolymer) its features include excellent non-stick properties, a low coefficient of friction and an operating temperature of up to 205°C [25–27].
- ETFE coatings (copolymer of ethylene and tetrafluoroethylene) with excellent chemical resistance, an operating temperature of up to 150°C , the highest strength of all fluoropolymers and the possibility to apply highly resistant coatings with a coating thickness of up to $500\ \mu\text{m}$ [28, 29].
- PEEK coatings (polyetheretherketone polymer) has exceptional mechanical properties, high chemical resistance, an operating temperature of up to 260°C and exceptional radiation resistance [30–32].
- PPS coatings (polyphenylenesulfide polymer) can operate at temperatures of up to 250°C , with high chemical resistance and good mechanical properties [33, 34].

A particular contribution to the development of release coatings are those based on fluoropolymers [35–37]. Fluoropolymers have been produced for a long time and are of great industrial

importance. They are characterised by high thermal and chemical resistance, an extremely low coefficient of friction and very favourable dielectric properties [24, 38]. From the moment the first fluoropolymers were obtained in DuPont's labs (in April 1938), their rapid expansion into almost all industries began. The reason for this was the remarkable properties [17, 24, 38–44]:

- Non-stickiness to other materials. The surface energy of fluoropolymers has the lowest value among all known solids. This characteristic determines many polymer properties such as wettability, adhesion and coefficient of friction. It is ideal for use as release coatings.
- Minimum friction coefficient. A coefficient of friction within the range $\mu = 0.05\text{--}0.2$ practically eliminates the phenomenon of "frictional oscillations", the so-called stick-slip effect. Static and kinetic friction coefficients are almost equal. The coefficient of friction is only slightly affected by temperature increases up to a value of 327°C .
- Thermal resistance. Fluoropolymer coatings are very good thermal insulators, with a high temperature resistance of up to 315°C . In the temperature range of $-200^\circ\text{C} \div +260^\circ\text{C}$, the coatings can be operated continuously without losing their properties.
- Chemical resistance. Fluoropolymer coatings are inert to the vast majority of chemicals, i.e.: acids, alkalis and organic solvents. Their resistance can be compared to that of precious metals. Fluoropolymers are resistant only to dissolved or molten lithium, gaseous fluorine and chlorotrifluorine.
- Dielectric properties. Fluoropolymer coatings have excellent insulating properties. Of all solid insulating materials, fluoropolymers have the lowest relative electrical permeability and dielectric loss factor.
- Physiological indifference. Many years of experience in the use of anti-adhesion coatings and toxicological studies have confirmed the complete safety of their use. Therefore, fluoropolymers are successfully used in the pharmaceutical industry and medicine.
- Anti-corrosion properties. Due to their physical and chemical properties, these coatings provide excellent protection against corrosion, even in aggressive environments.
- Non-wettability. Due to their low surface energy, the coatings exhibit low sorption and a high anti-adhesion coefficient.

The aim of this study was to evaluate the technology of surface preparation of steel samples in terms of anti-adhesive and mechanical properties through the use of polymer coatings. Such coatings are used in many industries, e.g. during the manufacture and operation of metal moulds [4, 5, 45–48] used, for example, in the production of resinous components. Then they facilitate the removal of components cast in, for example, epoxy or polymer resins from the moulds used to produce them. Considering the qualities of the available coatings and the economic aspect, PFA-type coatings were used in the study. Six variants of the technology for obtaining coatings with reduced release effects were used. Tests were then carried out to assess the energy status of the produced coatings by evaluating their wettability and determining the surface free energy. The next stage focused on evaluating the performance of the developed coatings. This research was divided into two stages. In the first, the mechanical properties of coatings applied to the surfaces of steel specimens subjected to three-point bending were assessed. The aim of this study was to assess the behaviour of the coating under the influence of deformations that may occur during the use of steel moulds and which may have a direct impact on the durability of the coating produced. For this purpose, the

quality of the produced coating was analysed after a three-point bending test, where the coating was subjected to deformations caused by compressive and tensile stresses. In the next step, the performance of the analysed coatings was evaluated in terms of durability and adhesion through a test performed in accordance with ASTM D3359 standard called the notch grid, a method of adhesion evaluation using the tape test or scratch test. In addition to the general purpose of assessing adhesion, this test gives information on the coating's resistance to scratches that may occur unintentionally during production processes.

RESEARCH METHODOLOGY

Material used in the study

The material used in the study was a DC01 sheet metal [49]. The samples to be tested were cut from sheet metal using LANTEK software according to the panel dimensions shown in Figures 1 and 2. The samples were cut using an Eckert model Combo portal hydro-abrasive cutting machine (Eckert AS Ltd, Legnica, Poland).

Garnet 80 mesh (Jet system, Elbląg, Poland) was used as an abrasive for cutting the sheets with the following technological parameters:

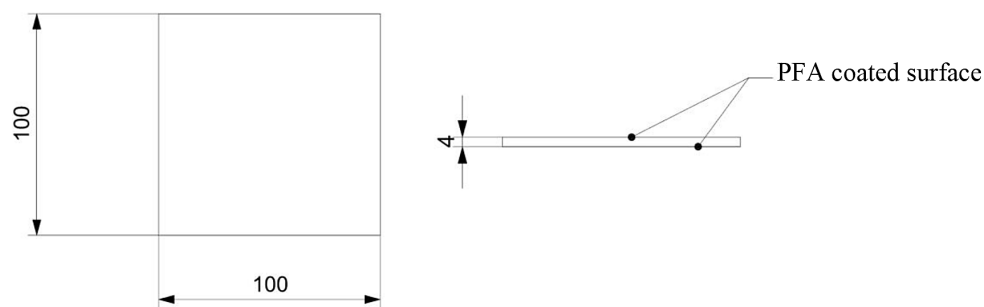


Fig. 1. Sample geometry for testing wetting angle and scratch test

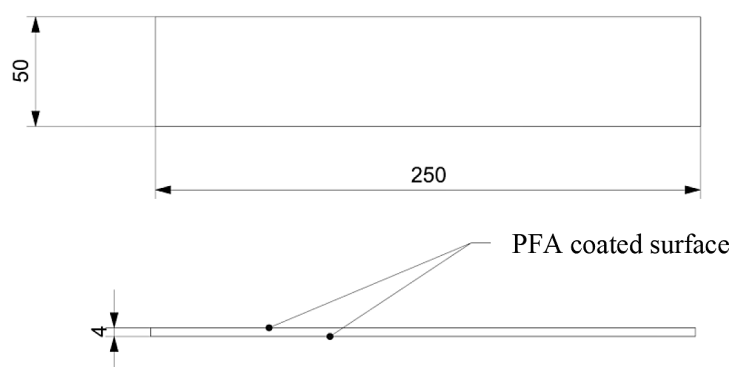


Fig. 2. Geometry of the samples to the three-point bend test

- water jet working pressure – $3500 \cdot 10^5$ Pa;
- abrasive flow – 0.45 kg/min;
- distance of nozzle from the cutting material – 3 mm;
- cutting speed – 200 mm/min.

After cutting, the metal samples were cleaned in a water stream washing away any abrasive residue and chips and then cleaned in a compressed air stream. The cut-out samples were subjected to a release coating process. The technological process for the application of anti-adhesive coatings used in the study consisted of several operations:

1. Operation of steel surface preparation by possible machining and application of primer.
2. Coating application operation.
3. Coating drying operation.
4. Coating curing operation.
5. Coating extended curing operation.

Six variants of PFA-type release coating technology were used in the study, differing in the number of operations and the parameters used. In each variant, the first operation was the same. First, each sample, over its entire surface, was machined with an abrasive tool of P180 gradation, so that a surface roughness denoted by the Ra parameter of $Ra = 3 - 4 \mu\text{m}$ was obtained, as required by

the PFA coating manufacturer. The surface quality of the machined samples was tested for surface roughness using a HOMMEL TESTER T1000 contact profilometer (HOMMEL-ETAMIC, Poznań, Poland). The surfaces of the samples were then degreased to remove physical and chemical contamination. Acetone was used for this purpose. The samples were degreased three times, with two wipes with a soft cloth, then sprayed thoroughly with a thin layer of acetone and allowed to evaporate. Table 1 shows the specification of the different coating technology variants used in the study.

The coating materials used in the tests were the basecoat with manufacturer’s designation 459G-643 PRIMER BLACK and the PFA coating material with designation 858G-110TOPCOAT CLEAR (Tetrachim, Noisiel, France). The base and coating layers were applied using an HVLP gun operating at an atomising air pressure of 0.2–0.3 MPa. The thickness of the PFA coatings was controlled using a Testan DT-25 FN (Testan, Gdańsk, Poland) thickness gauge to maintain dimensions within the recommended thickness ranges. The recommended DFT of the primer layer (final dry film thickness) should be 15-20 μm , while the recommended DFT of the PFA coating should be 35-75 μm . Five samples were prepared for each test using each of the surface preparation variants.

Table 1. Specification of individual coating technology variants

Operation	Coating process technology variant					
	Variant 1	Variant 2	Variant 3	Variant 4	Variant 5	Variant 6
Operation 1	Degreasing the surface of the sample sheet with acetone	Degreasing the surface of the sample sheet with acetone	Degreasing the surface of the sample sheet with acetone	Degreasing the surface of the sample sheet with acetone	Degreasing the surface of the sample sheet with acetone	Degreasing the surface of the sample sheet with acetone
Operation 2	Applying the primer and drying it for 15 minutes at a sample temperature of 250 °C	Applying the primer and drying it for 15 minutes at a sample temperature of 250 °C	Applying the primer and drying it for 15 minutes at a sample temperature of 250 °C	Applying the primer and drying it for 15 minutes at a sample temperature of 250 °C	Applying the primer and drying it for 15 minutes at a sample temperature of 250 °C	Applying the primer and drying it for 15 minutes at a sample temperature of 250 °C
Operation 3	PFA layer application, followed by drying for 15 minutes at 200 °C and curing for 20 minutes at 380 °C	PFA layer application, followed by drying for 15 minutes at 200 °C and curing for 20 minutes at 380 °C	PFA layer applied to the sample at 50 °C, then dried for 15 minutes at 200 °C and cured for 20 minutes at 380 °C	PFA layer applied to the sample at 150 °C, then dried for 15 minutes at 200 °C and cured for 20 minutes at 380 °C	PFA layer applied to the sample at 150 °C, then dried for 15 minutes at 200 °C and cured for 20 minutes at 380 °C	PFA layer applied to the sample at 150 °C, then dried for 15 minutes at 200 °C and cured for 20 minutes at 380 °C
Operation 4		Applying an additional layer of PFA, then drying it for 15 minutes at 200 °C and curing it for 20 minutes at 340 °C			Additional long heating for 3 hours at 340°C	Applying an additional layer of PFA, then drying it for 15 minutes at 200 °C and curing it for 20 minutes at 340 °C
Operation 5						Additional long heating for 3 hours at 340 °C

Test stand and tools

The coated samples were subjected to surface free energy (SFE) tests by measuring surface wetting angle, three-point bending and coatings adhesion.

The surface free energy was determined using the Owens-Wendt method, which is based on direct measurement of the wetting angle. Distilled water and diiodomethane CH₂I₂ were used as measurement fluids, with known values for the polar and dispersive components of the surface free energy, as shown in Table 2. The size of the droplet used was 4 μl. Fifteen replicate measurements were carried out on each sample. The results obtained and calculated are presented in the Table 3. These tests were carried out using a DSA30 goniometer (KRÜSS, Hamburg, Germany).

SFE calculations were made on the basis of the following formulae (1) [50, 53]:

$$\gamma_S = \gamma_S^d + \gamma_S^p \quad (1)$$

where:

$$(\gamma_S^d)^{0,5} = \frac{\gamma_d(\cos\theta_d+1) - \sqrt{\frac{\gamma_d^p}{\gamma_w^p}} \gamma_w(\cos\theta_w+1)}{2\left(\sqrt{\gamma_d^d} - \sqrt{\gamma_d^p \frac{\gamma_w^d}{\gamma_w^p}}\right)} \quad (2)$$

$$(\gamma_S^p)^{0,5} = \frac{\gamma_w(\cos\theta_w+1) - 2\sqrt{\gamma_S^d \gamma_w^d}}{2\sqrt{\gamma_w^p}} \quad (3)$$

- where: γ_S^d - dispersive part of the surface free energy of tested materials;
- γ_S^p - polar part of the surface free energy of the tested materials;
- γ_d - surface free energy of diiodomethane;
- γ_d^d - dispersive part of the diiodomethane surface free energy;
- γ_d^p - polar part of the diiodomethane surface free energy;
- γ_w - surface free energy of water;
- γ_w^d - dispersive part of the water surface free energy;
- γ_w^p - polar part of the water surface free energy.

Three-point bending tests were carried out on a Zwick/Roell Z2.5 testing machine, in accordance with PN-EN ISO 7438:2021-04 standard [54]. The crosshead speed during the test was 20 mm/min, while the initial test force was 5N and the distance between supports was 60 mm. Figure 3 shows how the test specimens were fixed in the testing machine. Both the tensile and compression sides of the specimen were assessed.

Table 2. Values of the polar and dispersive components of the SFE of water and diiodomethane [50–52]

Measuring liquids	Surface free energy of the measuring liquid γ_S	Dispersive component of the surface free energy of the measuring liquid γ^d	Polar component of the surface free energy of the measuring liquid γ^p
Distilled water	72.8 mJ/m ²	21.8 mJ/m ²	51.0 mJ/m ²
Diiodomethane	53.2 mJ/m ²	50.8 mJ/m ²	2.4 mJ/m ²

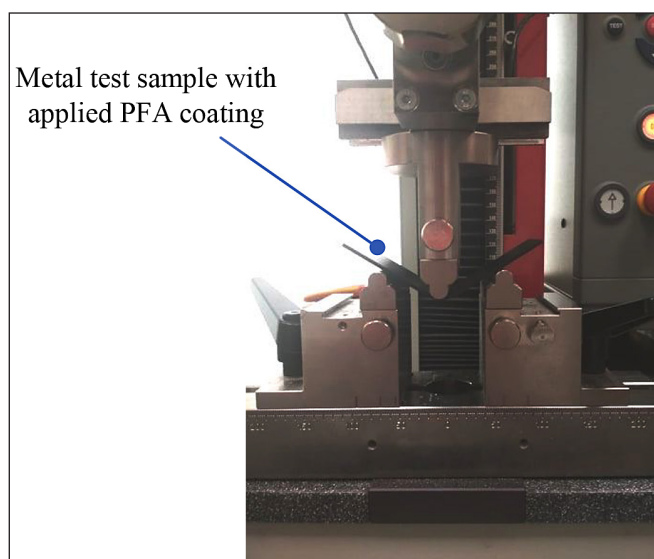


Fig. 3. Method of sample positioning during testing



Fig. 4. Toolkit for grid adhesion testing

Coating adhesion tests were carried out using the notch grid method. The tests were carried out in accordance with ASTM D3359-B standard [55] using a circular knife fitted with a 6x1 mm blade Elcometer 107 F10713348-6 (Elcometer, Manchester, United Kingdom). The tooling used is shown in Figure 4.

The incisions were made in the centre of the sample. The resulting images of the incision grid were evaluated organoleptically, but to increase the accuracy of the evaluation, surface images were taken using a DiGi Microscope Viting UM06 microscope (Vitiny, Kaohsiung, Taiwan).

RESULTS AND DISCUSSION

Surface free energy test by determining the wetting angle of a surface

Test results of the wetting angle measurement along with the calculated surface free energy are included in Table 3.

Table 4 shows examples of droplet photographs taken when wetting angle measurements were carried out.

The calculated surface free energy values allow the adhesion capacity of the surfaces under consideration to be determined. Figure 5 summarises the averaged calculated SEP values for each coating preparation variant of the analysed samples.

Analysing the obtained results of the surface free energy test, it can be observed that the lowest value of the surface free energy was obtained for series 6, while the highest value was obtained for series 1 and 3. This shows, therefore, that the characteristics of the surface coatings obtained for variant 6 are characterised to the highest degree by hydrophobic features, which may ensure their effective performance during application on the surfaces of steel moulds.

Three-point bending strength tests

A three-point bend test was carried out to determine the deformability of the coated

Table 3. Wetting angle averages and results of calculated SFE

Variant	Sample	Measuring liquid		SFE [mJ/m ²]	Variant	Sample	Measuring liquid		SFE [mJ/m ²]
		Diodomethane	Water				Diodomethane	Water	
		Wetting angle θ_d [°]	Wetting angle θ_w [°]				Wetting angle θ_d [°]	Wetting angle θ_w [°]	
Variant 1	1	87.3	94.3	17.33	Variant 2	1	87.7	108.2	14.50
	2	89.9	99.1	15.33		2	87.7	115.2	14.52
	3	89.9	89.6	19.18		3	89.7	111.6	13.45
	4	84.5	99.8	16.95		4	87.5	118.8	14.99
	5	86.9	92.3	18.51		5	86.6	116.8	15.26
Variant 3	1	91.6	90.2	18.61	Variant 4	1	89.6	99.4	15.33
	2	90.9	96.8	15.83		2	89.9	91.0	18.47
	3	92.0	94.8	16.38		3	90.1	110.1	13.34
	4	92.3	91.1	18.03		4	88.6	102.1	14.98
	5	93.3	94.5	16.28		5	90.3	95.1	16.68
Variant 5	1	96.9	107.2	11.34	Variant 6	1	98.1	107.7	10.92
	2	88.4	110.1	14.09		2	98.5	108.7	11.39
	3	96.1	110.3	11.06		3	97.8	107.2	11.10
	4	93.9	108.7	12.01		4	96.9	108.8	11.02
	5	94.5	105.9	12.29		5	97.4	109.9	10.72

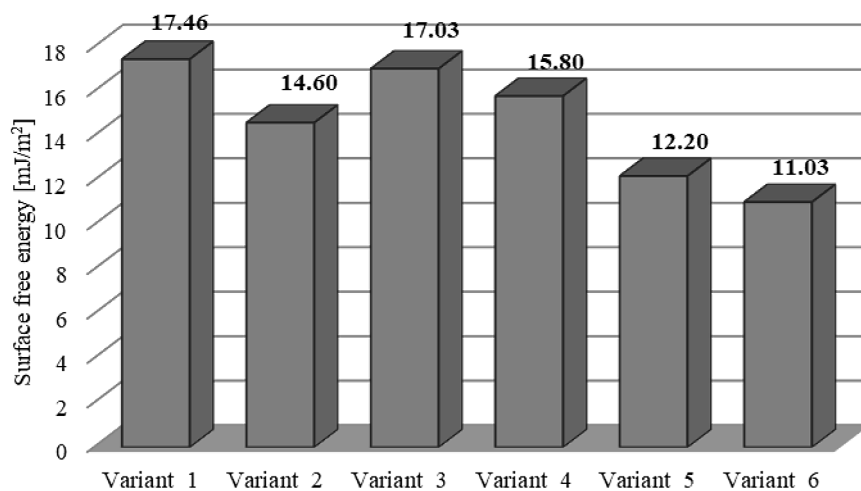


Fig. 5. Averaged surface free energy results for the applied anti-adhesive coating variants

Table 4. Photographs of a droplet of a wetting angle measurement of a surface with applied coatings according to the described variants

Variant	Droplet of wetting angle measurement with diiodomethane		Droplet measurement of wetting angle with water	
Variant 1				
Variant 2				
Variant 3				
Variant 4				
Variant 5				
Variant 6				

materials tested during forming and operation of the moulds. The results of the bending strength and photographs showing the appearance of the samples and their surfaces after the test are shown below.

The results of the recorded force and strain values for the different variants are included in Table 5. Figure 6 shows a sample of the curves obtained during the test (for variant 1).

The visible unevenness is due to the friction of the sample surface against the supports of the testing machine, on which they were positioned.

Statistical analysis was carried out to compare and establish differences between the results obtained. The assumption of normality of distribution and equality of variance was complied with, so parametric tests were used in the further stage of statistical analysis. The Tukey HSD test was used at an assumed significance level of $\alpha = 0.05$. A significance level of 0.05 is taken as the limit of acceptable error. The Tukey HSD test is a post-hoc (or multiple comparisons) test and can be used to determine the significance of differences between group averages in an analysis of variance

Table 5. Three-point bending test results

Variant	Sample	Maximum force F_M [N]	Deformation ϵ_M [mm]	Variant	Sample	Maximum force F_M [N]	Deformation ϵ_M [mm]
Variant 1	1	995	10.3	Variant 2	1	916	11.7
	2	916	11.0		2	914	11.8
	3	902	10.9		3	960	13.7
	4	939	14.9		4	967	15.1
	5	998	15.2		5	939	13.1
Average		950.0	12.5	Average		939.2	13.1
Standard deviation		44.5	2.38	Standard deviation		24.4	1.4
Variant 3	1	917	11.8	Variant 4	1	920	11.7
	2	920	11.2		2	906	11.2
	3	957	13.1		3	958	12.2
	4	965	13.7		4	952	13.6
	5	939	12.5		5	934	12.2
Average		939.6	12.5	Average		934.0	12.2
Standard deviation		21.5	1.0	Standard deviation		21.7	0.9
Variant 5	1	907	12.0	Variant 6	1	914	11.2
	2	903	11.1		2	911	11.2
	3	939	13.3		3	936	15.6
	4	949	15.7		4	940	13.6
	5	925	13.0		5	925	12.9
Average		924.6	13.0	Average		925.2	12.9
Standard deviation		19.9	1.73	Standard deviation		12.9	1.8

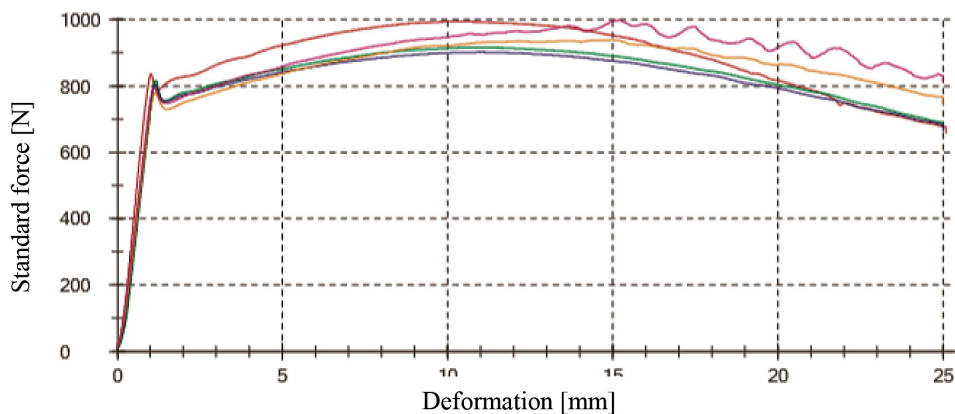


Fig. 6. Diagram of variant 1 coatings - standard force - deformation characteristics

Table 6. Tukey’s HSD test results for maximum force

Tukey's HSD test for F_M maximum force. Approximate probability for post hoc tests. Error: intergroup MS = 855.43, df = 19.000.						
	Variant 1	Variant 2	Variant 3	Variant 4	Variant 5	Variant 6
Variant 1		0.99	0.99	0.96	0.78	0.80
Variant 2	0.99		1.00	1.00	0.98	0.98
Variant 3	0.99	1.00		1.00	0.97	0.98
Variant 4	0.96	1.00	1.00		1.00	1.00
Variant 5	0.78	0.98	0.97	1.00		1.00
Variant 6	0.80	0.98	0.98	1.00	1.00	

Table 7. Tukey’s HSD test results for deformation

Tukey's HSD test for ϵ_M deformation. Approximate probability for post hoc tests. Error: MS between groups = 3.3381, df = 19.000.						
	Variant 1	Variant 2	Variant 3	Variant 4	Variant 5	Variant 6
Variant 1		1.00	1.00	1.00	1.00	1.00
Variant 2	1.00		1.00	0.98	1.00	1.00
Variant 3	1.00	1.00		1.00	1.00	1.00
Variant 4	1.00	0.98	1.00		0.98	0.99
Variant 5	1.00	1.00	1.00	0.98		1.00
Variant 6	1.00	1.00	1.00	0.99	1.00	

system. The results obtained from the Tukey HSD test are summarised in Tables 6 and 7.

The test results showed no significant differences in performance between the different coating variants analysed.

For completeness, Table 8 summarises the visual appearance of the surfaces of the samples after the bending test, from both the tension and compression sides. The resulting surfaces were subjected to organoleptic inspection.

On the tensile surface of the samples with the coating applied according to the parameters of variant 1, a slight detachment of the coating can be observed at the edge zones of the sample. There is saddle-shaped deformation – lifting of the outer edges. It can be concluded that this is the result of a complex stress state at the edges of the samples. In addition, microcracks can be seen at the bend of the specimen. On the side where the surface of the specimen was compressed, peeling of the coating is visible. The coating surface is visibly separated from the native material, but there is no coating damage on the surface.

On the tensile surface of the samples with the coating applied according to the parameters of variant 2, it is possible to observe, as in the case of the samples of series 1, a slight saddle-shaped deformation – lifting of the outer edges, but no

damage to the coating layer, apart from small microcracks indicating more the phenomenon of creep of the coating layer.

On the samples with the coating applied according to the parameters of variant 3, there were numerous coating surface defects. On samples where the coating surface was in tension, the coating surface deteriorated, cracking along the entire length of the protrusion created by bending the sample. Where the coating surface was in compression, numerous wrinkles and corrugations of the coating layer were observed. The samples in this series showed the least resistance of the coating to deformation during the forming-bending process of the modified surfaces.

On the tensile surface of the samples with the coating applied in accordance with the parameters of variant 4, a slight saddle-shaped deformation – lifting of the outer edges – can be observed and, as in the case of variant 2 samples, slight microcracking of the coating can be observed and, as in variant 1 samples, peeling of the material at the edges of the sample can be observed. Where the surface has been compressed, wrinkling of the coating can be seen, but this is relatively minor compared to, for example, the variant 3 samples.

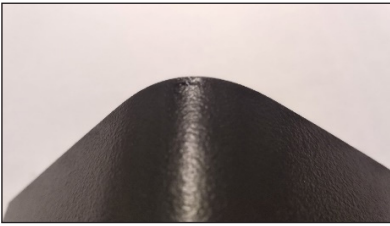
On the tensile surface of the samples with the coating applied according to the parameters of

variant 5, a slight deflection of the material at the edges of the sample can be observed, as in previous cases, but no surface defects were observed. Very slight wrinkling of the coating is visible on the compressed surface. One sample showed a single bubble not exceeding 2 mm in length.

For the samples with the coating applied according to the parameters of variant 6, no

coating surface defects were observed. On the samples where the surface was in tension, only a slight saddle-shaped deformation – lifting of the outer edges – can be observed, as in the case of samples of all series, but no damage to the coating layer occurred. In the case of the compressed surface, no damage to the coating was observed.

Table 8. Surface appearance of coated samples after three-point bending test

Coating preparation variant	Appearance of the tensile surface	Appearance of the compression surface
Variant 1		
Variant 2		
Variant 3		
Variant 4		
Variant 5		
Variant 6		

Tests for measuring coating adhesion using the notch grid method

According to the above-mentioned standard, the following interpretation of the notched line results is possible [55]:

- 5B – The edges of the notches are smooth, no square of the coating from the notch grid has been torn off.
- 4B – Only small flakes of the shell on the edges of the incision grid detached. No square of the rectangular notch grid has been torn off. The total area of the damaged coating is no more than 5%.
- 3B – Coating falls off in small flakes along grid lines and visible cracks and detachment of small pieces of coating between grid lines. Total area of damage greater than 5% but not exceeding 15%.
- 2B – The coating falls off in flakes along the notches partly or entirely in the form of long ribbons and/or breaks off in flakes partly or entirely from the squares of the notch grid. Area of damage greater than 15% and less than 35%.
- 1B – The coating falls off in flakes along the notches in the form of long ribbons and/or flakes off in part or whole from the squares of the notch grid. Area of damage greater than 35% and less than 65%.
- 0B – Each degree of coating detachment that cannot be classified as 1B.

On this basis, it can be assumed that the best properties in terms of adhesion of the coating to the substrate are those whose results can be categorised as group 5B. The results of the coating adhesion test are presented in Table 9.

If there was any doubt about the evaluation of the results obtained and their classification into a specific result group, the photographs taken were analysed in more detail using ImageJ, an image processing and analysis programme. An example of the programme window with the analysis performed is shown in Figure 7.

On the basis of the scratch test results obtained, it can be clearly stated that the best properties in terms of adhesion and scratch resistance were demonstrated by the samples made according to the technology applied in variant 6.

Table 10 presents the cumulative results of the individual tests to which the coatings were subjected and ranks the results obtained in such a way that they represent the results from the best (green) through standard (blue) to the worst solution (red), with the number 1 indicating the best solution and 6 the worst solution. The smallest total score indicates the best option.

On the basis of the variants of coating preparation technology used, it can be seen that, as a result of the verification of their properties, the best characteristics were variant 6, which consisted in the modification of the standard procedure in the application of the coating by applying an additional layer of PFA and its prolonged heating.

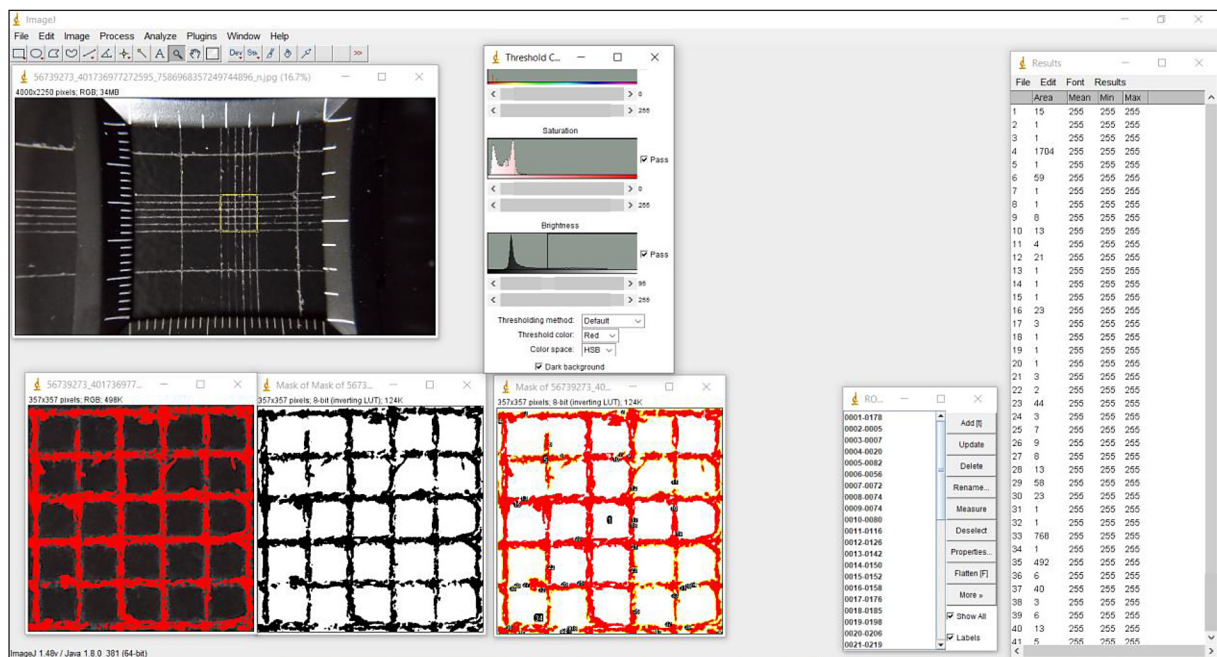


Fig. 7. ImageJ interface window with example image analysis

Table 9. Results of the test for adhesion of coatings using the notch grid method

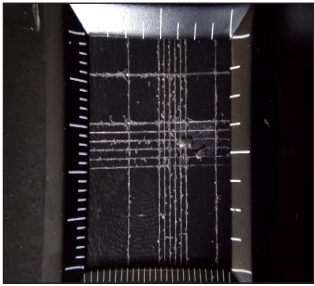
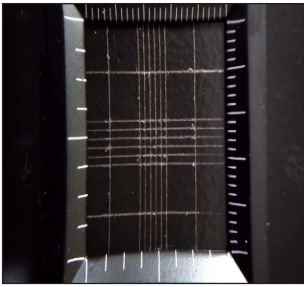
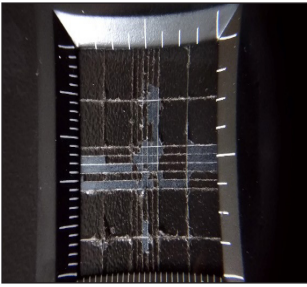
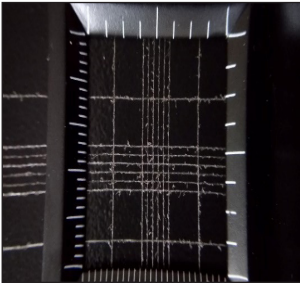
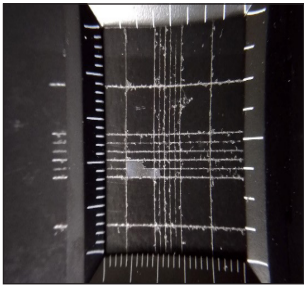
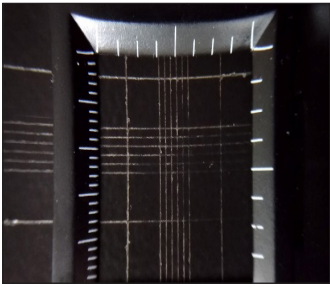
Variant	Example photo of a surface	Sample No.	Adhesion assessment according to ASTM D3359-B standard
Variant 1		1	2B
		2	4B
		3	4B
		4	4B
		5	3B
Variant 2		1	4B
		2	4B
		3	5B
		4	4B
		5	4B
Variant 3		1	0B
		2	0B
		3	0B
		4	0B
		5	0B
Variant 4		1	4B
		2	4B
		3	4B
		4	4B
		5	3B
Variant 5		1	4B
		2	4B
		3	4B
		4	4B
		5	3B
Variant 6		1	5B
		2	4B
		3	4B
		4	5B
		5	5B

Table 10. Results of the classification of the developed coating variants in terms of the test methods used

Type of test	Variant 1	Variant 2	Variant 3	Variant 4	Variant 5	Variant 6
Surface free energy	6	3	5	4	2	1
Three-point bending	5	4	6	3	2	1
Measurement of coating adhesion	4	2	6	3	3	1
Total score	15	9	17	10	7	3

CONCLUSIONS

Based on the results obtained from the research, the following conclusions can be established:

- The lowest value of surface free energy was obtained for variant 6 of surface preparation, while the highest value was obtained for variants 1 and 3. The surface coating characteristics obtained for variant 6 on the basis of SEP are characterised to the highest degree by hydrophobic features.
- The results of the three-point bending strength test did not show any significant differences in the results in terms of forces, which attests to the repeatability of the material characteristics exhibited by the DC01 sheet used, but the tests did allow the susceptibility of the coated surfaces to moulding during the bending process and in their service life to be assessed. The best results were obtained for specimens to which coatings were applied according to the parameters of variants 5 and 6, while the worst results were obtained for variant 3. The deformations and their nature attest to the fact that steel moulds with PFA coatings applied to them should not work in compression and should be avoided for them.
- The results of the adhesion test using the grid method showed that the surfaces of the samples with the coating applied according to the technology adopted in variant 3 performed worst in the test, while the samples of series 2 and 6 performed best. During the tests carried out, in the case of the samples made according to variant 1, both in the bending test and during the adhesion test using the grid method, one of the samples showed completely different properties, the surface was damaged. This may be indicative of a lack of repeatability and stability during the coating process with the respective method. The best adhesion and scratch resistance properties were demonstrated by specimens of series 6.

REFERENCES

1. Paz-Gómez, Caño-Ochoa, Rodríguez-Alabanda, Romero, Cabrerizo-Vílchez, Guerrero-Vaca, i in. Water-Repellent Fluoropolymer-Based Coatings. *Coatings*. 2019;9(5):293.
2. Darolia R. Thermal barrier coatings technology: critical review, progress update, remaining challenges and prospects. *International Materials Reviews*. 2013;58(6):315–48.
3. Arshad A, Yajid MAM, Idris MH. Microstructural characterization of modified plasma spray LZ/YSZ thermal barrier coating by laser glazing. *Materials Today: Proceedings*. 2021;39:941–6.
4. Critchlow GW, Litchfield RE, Sutherland I, Grandy DB, Wilson S. A review and comparative study of release coatings for optimised adhesion in resin transfer moulding applications. *International Journal of Adhesion and Adhesives*. 2006;26(8):577–99.
5. Ruiz-Cabello FJM, Rodríguez-Criado JC, Cabrerizo-Vílchez M, Rodríguez-Valverde MA, Guerrero-Vacas G. Towards super-nonstick aluminized steel surfaces. *Progress in Organic Coatings*. 2017;109:135–43.
6. Sánchez-Urbano F, Paz-Gómez G, Rodríguez-Alabanda Ó, Romero P, Cabrerizo-Vílchez M, Rodríguez-Valverde M, i in. Non-Stick Coatings in Aluminium Molds for the Production of Polyurethane Foam. *Coatings*. 2018;8(9):301.
7. Rossi S, Gai G, De Benedetto R. Functional and perceptive aspects of non-stick coatings for cookware. *Materials & Design*. 2014;53:782–90.
8. Ashokkumar S, Adler-Nissen J, Møller P. Factors affecting the wettability of different surface materials with vegetable oil at high temperatures and its relation to cleanability. *Applied Surface Science*. 2012;263:86–94.
9. Bouaidat S, Berendsen C, Thomsen P, Petersen SG, Wolff A, Jonsmann J. Micro patterning of cell and protein non-adhesive plasma polymerized coatings for biochip applications. *Lab Chip*. 2004;4(6):632.
10. Costa EC, De Melo-Diogo D, Moreira AF, Carvalho MP, Correia IJ. Spheroids Formation on Non-Adhesive Surfaces by Liquid Overlay Technique: Considerations and Practical Approaches. *Biotechnol J*. 2018;13(1):1700417.

11. Tracton AA, redaktor. Coatings materials and surface coatings. Boca Raton, FL: CRC Press; 2007. 1 s.
12. Friz M, Waibel F. Coating Materials. W: Kaiser N, Pulker HK. Optical Interference Coatings. Berlin, Heidelberg: Springer Berlin Heidelberg; 2003. s. 105–30. (Rhodes WT. Springer Series in Optical Sciences; t. 88).
13. Rudawska A, Miturska-Barańska I, Doluk E. Influence of Surface Treatment on Steel Adhesive Joints Strength—Varnish Coats. *Materials*. 2021;14(22):6938.
14. Zhao Q, Wang C, Liu Y, Wang S. Bacterial adhesion on the metal-polymer composite coatings. *International Journal of Adhesion and Adhesives*. 2007;27(2):85–91.
15. Smith JR, Lamprou DA. Polymer coatings for biomedical applications: a review. *Transactions of the IMF*. 2014;92(1):9–19.
16. Feng W, Patel SH, Young MY, Zunino JL, Xanthos M. Smart polymeric coatings—recent advances. *Adv Polym Technol*. 2007;26(1):1–13.
17. S.N. Raman, Nguyen T, Mendis P. A Review on the Use of Polymeric Coatings for Retrofitting of Structural Elements against Blast Effects. *EJSE*. 2011;11:69–80.
18. Schellenberger F, Encinas N, Vollmer D, Butt HJ. How Water Advances on Superhydrophobic Surfaces. *Phys Rev Lett*. 2016;116(9):096101.
19. Liu Y, Song D, Choi CH. Anti- and De-Icing Behaviors of Superhydrophobic Fabrics. *Coatings*. 2018;8(6):198.
20. Fürstner R, Barthlott W, Neinhuis C, Walzel P. Wetting and Self-Cleaning Properties of Artificial Superhydrophobic Surfaces. *Langmuir*. 2005;21(3):956–61.
21. Dhanumalayan E, Joshi GM. Performance properties and applications of polytetrafluoroethylene (PTFE)—a review. *Adv Compos Hybrid Mater*. 2018;1(2):247–68.
22. Yingying Zhang, Qilin Zhang, Chuanzhi Zhou, Ying Zhou. Mechanical properties of PTFE coated fabrics. *Journal of Reinforced Plastics and Composites*. 2010;29(24):3624–30.
23. Xu K, Yang Z, Sun W, Wang L, Fan J, Zhang H, i in. Acid permeability related corrosion protection properties of PTFE coatings for waste heat recovery. *Corrosion Science*. 2023;218:111141.
24. He Y, Farokhzadeh K, Edrisy A. Characterization of Thermal, Mechanical and Tribological Properties of Fluoropolymer Composite Coatings. *J of Materi Eng and Perform*. 2017;26(6):2520–34.
25. Leivo E, Wilenius T, Kinos T, Vuoristo P, Mäntylä T. Properties of thermally sprayed fluoropolymer PVDF, ECTFE, PFA and FEP coatings. *Progress in Organic Coatings*. 2004;49(1):69–73.
26. Barhoumi N, Khelifi K, Maazouz A, Lamnawar K. Fluorinated Ethylene Propylene Coatings Deposited by a Spray Process: Mechanical Properties, Scratch and Wear Behavior. *Polymers*. 2022;14(2):347.
27. Song HJ, Zhang ZZ. Study on the tribological and hydrophobic behaviors of phenolic coatings reinforced with PFW, PTFE and FEP. *Surface and Coatings Technology*. 2006;201(3–4):1037–44.
28. Hu J, Chen W, Zhao B, Yang D. Buildings with ETFE foils: A review on material properties, architectural performance and structural behavior. *Construction and Building Materials*. 2017; 131:411–22.
29. Lamnatou Chr, Moreno A, Chemisana D, Reitsma F, Clariá F. Ethylene tetrafluoroethylene (ETFE) material: Critical issues and applications with emphasis on buildings. *Renewable and Sustainable Energy Reviews*. 2018;82:2186–201.
30. Zhang G, Liao H, Yu H, Ji V, Huang W, Mhaisalkar SG, i in. Correlation of crystallization behavior and mechanical properties of thermal sprayed PEEK coating. *Surface and Coatings Technology*. 2006;200(24):6690–5.
31. Hou X, Shan CX, Choy KL. Microstructures and tribological properties of PEEK-based nanocomposite coatings incorporating inorganic fullerene-like nanoparticles. *Surface and Coatings Technology*. 2008;202(11):2287–91.
32. Zhang C, Zhang G, Ji V, Liao H, Costil S, Coddet C. Microstructure and mechanical properties of flame-sprayed PEEK coating remelted by laser process. *Progress in Organic Coatings*. 2009;66(3):248–53.
33. Wang H, Yan L, Gao D, Liu D, Wang C, Sun L, i in. Tribological properties of superamphiphobic PPS/PTFE composite coating in the oilfield produced water. *Wear*. 2014;319(1–2):62–8.
34. Xu H, Feng Z, Chen J, Zhou H. Tribological behavior of the carbon fiber reinforced polyphenylene sulfide (PPS) composite coating under dry sliding and water lubrication. *Materials Science and Engineering: A*. 2006;416(1–2):66–73.
35. Al GGH et. Fluoropolymers 2: Properties. Dordrecht: Springer; 1999.
36. Sales J, Schlipf M, Kapoor D. Critical Use of Fluoropolymers in the Functioning of Modern Society. *International Chemical Regulatory & Law Review*. 2023;6(1).
37. Quéré D, Reyssat M. Non-adhesive lotus and other hydrophobic materials. *Phil Trans R Soc A*. 2008;366(1870):1539–56.
38. Tamir E, Sidess A, Srebnik S. Thermodynamic, structural, and mechanical properties of fluoropolymers from molecular dynamics simulation:

- Comparison of force fields. *Chemical Engineering Science*. 2019;205:332–40.
39. Li XW, Song RG, Jiang Y, Wang C, Jiang D. Surface modification of TiO₂ nanoparticles and its effect on the properties of fluoropolymer/TiO₂ nanocomposite coatings. *Applied Surface Science*. 2013;276:761–8.
 40. Bhairamadgi NS, Pujari SP, Van Rijn CJM, Zuilhof H. Adhesion and Friction Properties of Fluoropolymer Brushes: On the Tribological Inertness of Fluorine. *Langmuir*. 2014;30(42):12532–40.
 41. Wang Z, Zuilhof H. Antifouling Properties of Fluoropolymer Brushes toward Organic Polymers: The Influence of Composition, Thickness, Brush Architecture, and Annealing. *Langmuir*. 2016;32(26):6571–81.
 42. Kłonica M, Kuczmaszewski J. Modification of Ti6Al4V Titanium Alloy Surface Layer in the Ozone Atmosphere. *Materials*. 2019;12(13):2113.
 43. Szabelski J. Effect of incorrect mix ratio on strength of two component adhesive Butt-Joints tested at elevated temperature. Stančková D, Vaško M, Rudawska A, Čuboňová N, Sapietová A, Mrázik J, i in. *MATEC Web Conf*. 2018;244:01019.
 44. Szabelski J, Karpiński R, Jonak J, Frigione M. Adhesive Joint Degradation Due to Hardener-to-Epoxy Ratio Inaccuracy under Varying Curing and Thermal Operating Conditions. *Materials*. 2022;15(21):7765.
 45. Zhao Q, Liu Y. Modification of stainless steel surfaces by electroless Ni-P and small amount of PTFE to minimize bacterial adhesion. *Journal of Food Engineering*. 2006;72(3):266–72.
 46. Kłonica M. Analysis of the effect of selected factors on the strength of adhesive joints. *IOP Conf Ser: Mater Sci Eng*. 2018;393:012041.
 47. Kłonica M. Application of the Ozonation Process for Shaping the Energy Properties of the Surface Layer of Polymer Construction Materials. *J Ecol Eng*. 2022;23(2):212–9.
 48. Karpiński, Szabelski, Maksymiuk. Seasoning Polymethyl Methacrylate (PMMA) Bone Cements with Incorrect Mix Ratio. *Materials*. 2019;12(19):3073.
 49. PN-EN 10130:2009 - Cold-rolled flat products of low carbon steels for cold forming.
 50. Park SJ, Cho MS, Lee JR. Studies on the Surface Free Energy of Carbon–Carbon Composites: Effect of Filler Addition on the ILSS of Composites. *Journal of Colloid and Interface Science*. 2000;226(1):60–4.
 51. Baldan A. Adhesion phenomena in bonded joints. *International Journal of Adhesion and Adhesives*. 2012;38:95–116.
 52. Miturska-Barańska I, Józwick J, Bere P. Effect of Face Milling Parameters of Carbon Fiber Reinforced Plastics Composites on Surface Properties. *Adv Sci Technol Res J*. 2022;16(2):26–38.
 53. Miturska-Barańska I, Rudawska A, Doluk E. The Influence of Sandblasting Process Parameters of Aerospace Aluminium Alloy Sheets on Adhesive Joints Strength. *Materials*. 2021;14(21):6626.
 54. PN-EN ISO 7438:2021-04 - Metals - Bending test.
 55. ASTM D3359-22 - Standard Test Methods for Rating Adhesion by Tape Test.